ELSEVIER

Reactive template assisted growth of one-dimensional nanostructures of titanium dioxide

Yao-An Chung [a], Chi-Young Lee [b], Chih-Wei Peng [a,c], Hsin-Tien Chiu [a,*]

[a] *Department of Applied Chemistry, National Chiao Tung University, Hsinchu 30050, Taiwan, ROC*
[b] *Department of Materials Science and Engineering and Materials Science Center, National Tsing Hua University, Hsinchu 30043, Taiwan, ROC*
[c] *Institut des Matériaux Jean Rouxel, Laboratoire de Physique Cristalline, 2 rue de la Houssinière, BP 32229, 44322 Nantes Cedex 3, France*

Abstract

$TiCl_4$ was employed to react with the reactive template Na@AAO, Na inside the channels of anodic aluminum oxide membranes, followed by O_2 oxidation at 623 K and annealed at 723 and 873 K to form one-dimensional nanostructures of TiO_2. Free standing polycrystals of anatase TiO_2 (diameter = 200–400 nm, length = 60 μm) were obtained after the template was removed.
© 2006 Elsevier B.V. All rights reserved.

Keywords: Oxides; Nanostructures; Chemical synthesis

Due to the photocatalytic activity, remarkable size effect and other properties, titanium dioxide (TiO_2) nanostructures are widely investigated for applications in photovoltaic cells [1], semiconductor photo-catalysts [2], and gas sensors [3]. Before, TiO_2 has been fabricated into one-dimensional (1D) structures via various solution methods [4–23]. In many cases, anodic aluminum oxide (AAO) was used as the templates to assist structure formation [11–23]. Recently, we demonstrated a novel "reactive template" strategy to fabricate carbon nanotubes [24]. The reaction employed Na@AAO, sodium inside the channels of AAO, as the reactive template to react with the vapor of C_6Cl_6 at elevated temperatures. Here, we wish to report the application of the reactive template strategy to synthesize arrays of one-dimensional nanostructures of TiO_2.

In a typical reaction, the reactive template, Na@AAO was prepared by pyrolyzing of NaH (0.20 g, 8.3 mmol, Aldrich) on AAO (Whatman Anodisc 13, pore diameter of 200 nm, thickness of 60 μm) at 623 K for 1 h under an Ar atmosphere inside a tube furnace [24]. The as prepared Na@AAO was reacted with $TiCl_4$ (99%, Aldrich), maintained at 298 K under a constant flow of Ar (10 sccm), at 623 K for 20 h to generate a black product. The as prepared product was further oxidized by O_2 at 623 K for 2 h followed by annealing at 723–873 K for 1 h to generate a white product. The as prepared product was dipped into 6 M NaOH for 10–60 min to remove the AAO template. Finally, the products were filtered, rinsed with distilled water and dried at 373 K in air. In Table 1, experimental data of two representative examples of the reaction products are summarized. Sample A was annealed at 723 K followed by being immersed in 6 M NaOH. Because A appeared to be unstable in the solution, it was treated for only 10 min in it. While sample B, which was thermally treated at 873 K, appeared to be more stable in the solution and an extended treatment of 1 h was applied to remove all AAO.

Scanning electron microscopic (SEM, JEOL JSM-6330F) images and energy dispersive spectroscopy (EDS) data of A and B are shown in Fig. 1. The AAO assisted both A and B to form well-aligned 1D nanostructures. The average diameters of A and B are ca. 300–400 nm and 200–300 nm, as shown in Fig. 1a and b, respectively. A has a wall structure constructed by thin nanosheets while B is constructed by nanoparticles. Because A was less stable in the basic solution, only a short treatment in NaOH was applied. The EDS data listed in Table 1 suggest that A, which was immersed for only 10 min, has a much higher Al/Ti ratio than that of B, which was treated for 60 min in NaOH. The high Al concentration of A suggests that the AAO template was yet to be removed completely. Fig. 2 shows transmission electron microscopic (TEM, Philips TECNAI 20 operated at 200 keV) images and electron diffraction (ED) patterns of A and B. The images shown in Fig. 2a–d reveal that the observed nanostructures of A and B, nanosheets and nanoparticles, respec-

* Corresponding author. Tel.: +886 3 5731514; fax: +886 3 5723764.
E-mail address: htchiu@cc.nctu.edu.tw (H.-T. Chiu).

Table 1
Summary of experimental data for TiO$_2$ 1D nanostructure preparation

Sample	Annealing temperature (K)	Dipping time in 6 M NaOH (min)	Color	Morphology by SEM	Isolated quantity	EDS (at. %)	ED	XRD	Raman
A	723	10	White	1D structures of nanosheets	Low	Ti 6 Al 14 O 80	Anatase TiO$_2$	Anatase TiO$_2$ Rutile TiO$_2$ Al$_2$O$_3$ (minor)	Anatase TiO$_2$
B	873	60	White	1D structures of nanoparticles	High	Ti 22 Al 1 O 77	Anatase TiO$_2$	Anatase TiO$_2$ Rutile TiO$_2$ Al(OH)$_3$ (minor)	Anatase TiO$_2$ (major) Rutile TiO$_2$ (minor)

tively, are consistent with the SEM images shown in Fig. 1. The ED patterns of A and B, shown in the insets of Fig. 2a and c, respectively, are indexed to the ring pattern of anatase TiO$_2$ in Fig. 2e. In Fig. 3, the X-ray diffraction (XRD, BRUKER AXS D8 ADVANCE with Cu Kα radiation) study data suggest that the major components of A are anatase TiO$_2$ (JCPDF 21-1272) and rutile TiO$_2$ (JCPDF 21-1276). Reflections from traces of unremoved Al$_2$O$_3$ (JCPDF 74-2206) are observed in

Fig. 1. SEM and EDS of TiO$_2$ nanostructures prepared at 623 K. (a) Sample A: annealed at 723 K and dipped in 6 M NaOH for 10 min. (b) Sample B: annealed at 873 K and dipped in 6 M NaOH for 60 min.

the XRD pattern too. The XRD pattern of B is also composed of reflections from both anatase and rutile TiO$_2$. In addition, some minute quantities of Al$_2$O$_3$ and Al(OH)$_3$ (JCPDF 33-0018) are observed. Raman (Jabin-Yvon Raman Spectrometer T-64000, incident wavelength at 514.5 nm, 20 mW at sample) spectra of A and B are shown in Fig. 4. In the spectrum of A, six active fundamental modes are observed and assigned to the vibrations of anatase TiO$_2$. These are 144 cm^{-1} (E_g), 197 cm^{-1} (E_g), 397 cm^{-1} (B_{1g}), 518 cm^{-1} (A_{1g} and B_{1g}, unresolved) and 640 cm^{-1} (E_g). For B, three additional bands of rutile TiO$_2$ are detected at 144 cm^{-1} (B_{1g}), 448 cm^{-1} (E_g) and 613 cm^{-1} (A_{1g}). B also shows a set of multiple peaks near 230 cm^{-1}. As discussed in literature, this observation is attributed to the result of a second-order process [25,26].

There are several apparently inconsistent observations. First of all, although the Raman study suggests that A is mostly anatase, the XRD shows reflections from both anatase and rutile phases. The anatase signals appear to be weak while, comparatively; the rutile signals seem to be strong. This suggests that the anatase TiO$_2$ in A could either be small in size or did not crystallize well because the overall process was carried out at relatively low temperatures. Origin of the rutile formation will be discussed below. Another intriguing point is that both anatase and rutile TiO$_2$ can be observed by XRD and Raman but in the 1D nanostructure observed by TEM, only anatase is detected by ED for both A and B. The discrepancy suggests that only anatase TiO$_2$ was formed inside the confined AAO channels under the reaction conditions employed. On the other hand, rutile TiO$_2$, the thermodynamically more stable phase [27], appeared to be formed from the reaction between TiCl$_4$ and Na outside the AAO template. A preliminary investigation showed that under comparable conditions, a direct reaction between TiCl$_4$ and Na alone, followed by O$_2$ oxidation generated rutile instead of anatase TiO$_2$ particles as the major product. The reason for this phenomenon will be discussed below.

In Scheme 1, employing the reactive template Na@AAO to fabricate the 1D nanostructures of TiO$_2$ is summarized. First, Na@AAO is formed by filling the AAO channels with Na liquid, the product of thermolysis of NaH. In actual experiments, there was always some Na did not flow into the channels. Next, by passing TiCl$_4$ vapor over Na@AAO, generation of (Ti + NaCl)@AAO, nanosized metallic Ti and NaCl inside the AAO channels, is suggested. Also, formation of freestanding nanosized metallic Ti from the reaction between TiCl$_4$ and
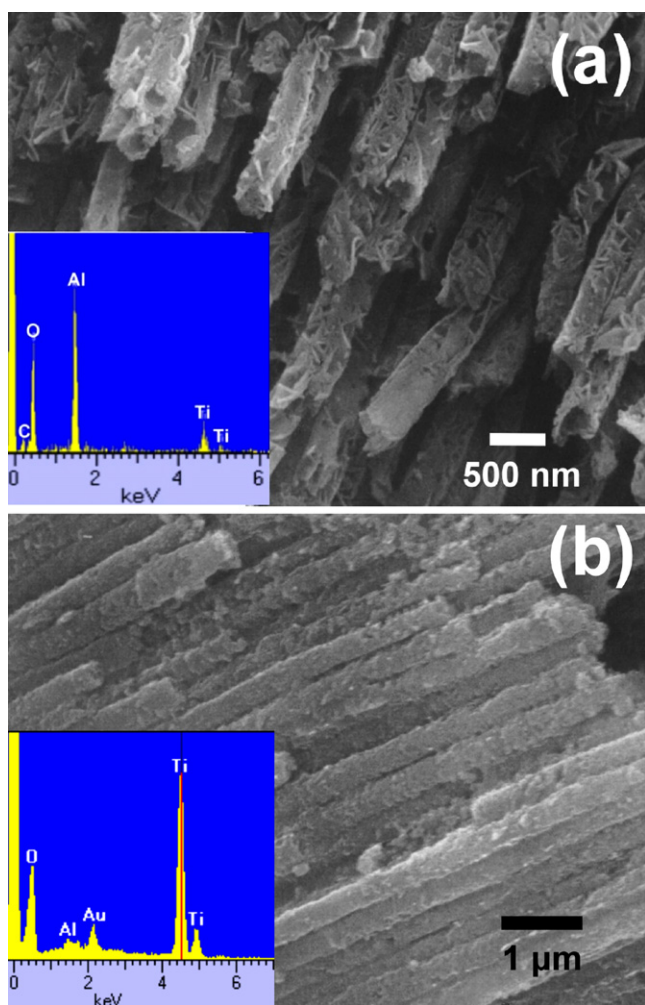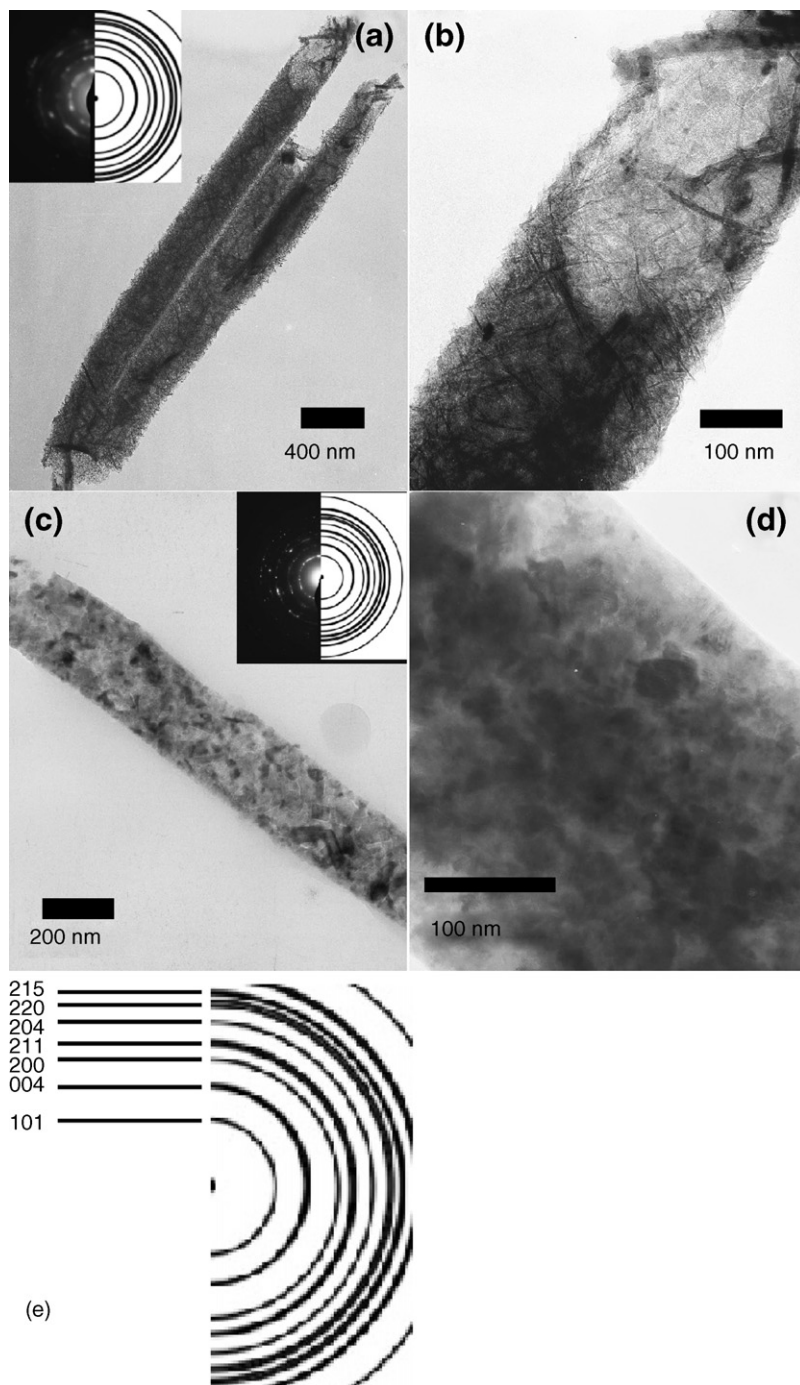
Fig. 2. TEM and ED of TiO_2 nanostructures. (a) Image of sample A; (b) high-magnification image from (a); (c) image of sample B; (d) high-magnification image from (c); (e) simulated ED pattern of anatase TiO_2.

Na outside the AAO template can be anticipated. Isolating the nanostructured metallic Ti from AAO were attempted but yet to be achieved successfully. The difficulty was due to the high reactivity of nanosized Ti towards air and moisture. Then, as shown in the scheme, after (Ti + NaCl)@AAO is oxidized by O_2, $(TiO_2 + NaCl)$@AAO is formed. In the actual experiments discussed above, in addition to anatase crystals, which grew inside the AAO channels, rutile crystals also formed outside the template. The origin for this is rationalized as follows. Due to the

high aspect ratio of the template channels, O_2 cannot diffuse easily to react with the Ti nanoparticles formed inside AAO. As the reaction rate is restricted by O_2 diffusion, the rate of heat released from the oxidation process is limited. The heat could dissipate to the environment quickly so that the local temperature is maintained during the reaction. The consequence is that even though the reaction between Ti and O_2 is expected to be highly exothermic, the standard Gibbs free energy of reaction $(\Delta G_r^\circ) = -889.5$ mol per mole of TiO_2 formed [28], the local
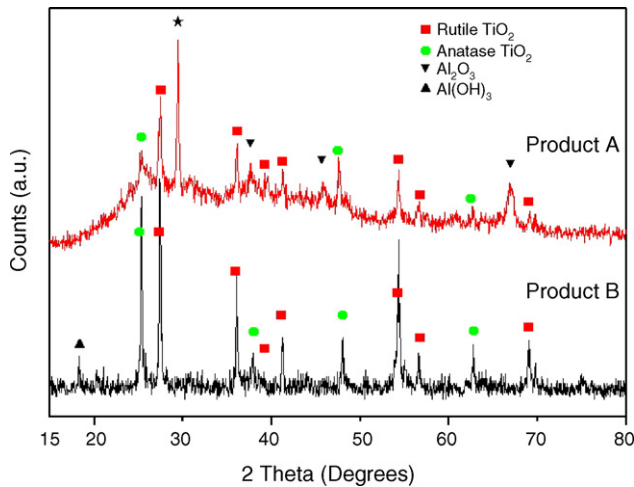
Fig. 3. XRD spectrum of TiO$_2$ nanostructures prepared at 623 K. Sample A, annealed at 723 K and dipped in 6 M NaOH for 10 min; Sample B, annealed at 873 K and dipped in 6 M NaOH for 60 min.
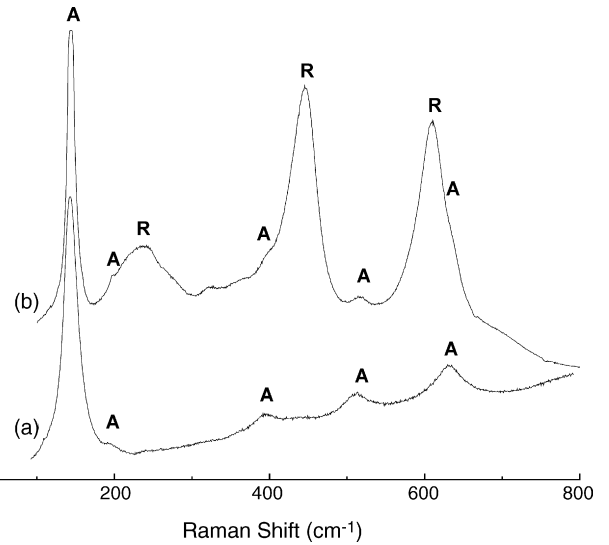

Fig. 4. Micro-Raman spectra of (a) A and (b) B. A: anatase; R: rutile.

temperature inside AAO does not raise significantly. The condition is suitable for the as-formed TiO$_2$ to crystallize into anatase. On the other hand, for the oxidation process outside the AAO channels, the diffusion of O$_2$ should be fast and the heat releasing is concentrated in a brief period of time. This would raise the local temperature so that the oxide can crystallize into the high temperature stable rutile phase. This explains why rutile formed outside the template while anatase was shaped into the 1D structure by the AAO. Finally, in the last step shown in the scheme, NaCl and AAO are removed in a NaOH solution to offer the 1D arrays of TiO$_2$. The annealing temperature appears to play an important role in the process. It affected the crystallinity, the

morphology, and the reactivity of TiO$_2$ towards the AAO template and the NaOH solution. Annealed at 723 K, the 1D TiO$_2$ product of A dissolved quickly by the NaOH solution as the AAO was etched away. On the other hand, the 1D TiO$_2$ product of B, annealed at 873 K, grew into better crystals and resisted the NaOH solution better. Consequently, to isolate the 1D product B, an extended NaOH dipping time was needed to remove the AAO template. At an annealing temperature of 1073 K, the AAO template was found to be extremely difficult to remove by the NaOH solution. We suggest that at this temperature, interdiffusion of Ti and Al atoms became more important and stronger adhesion between TiO$_2$ and AAO was formed.
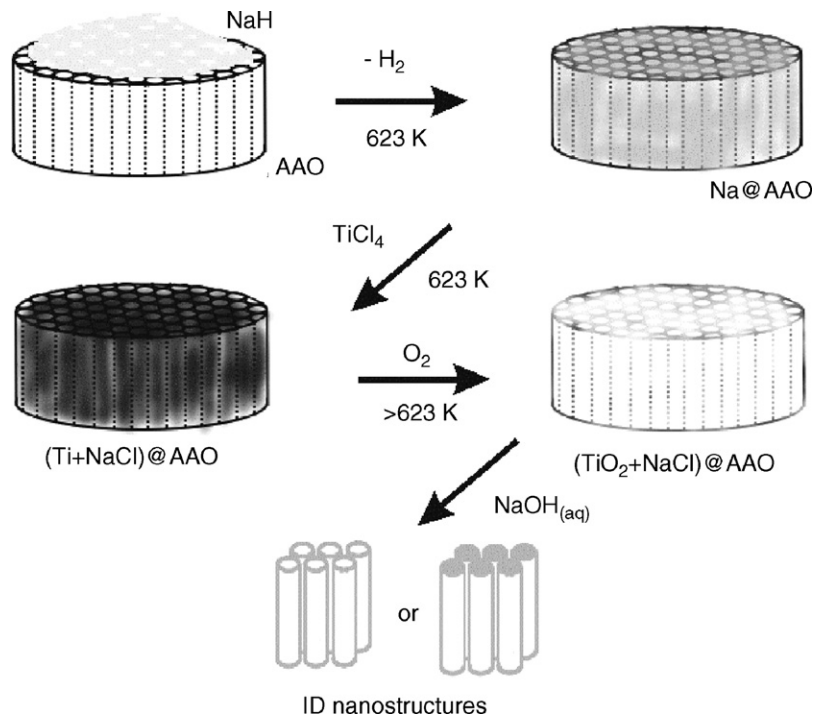
Scheme 1. Reaction steps to synthesize 1D nanostructures of TiO$_2$.

In conclusion, we have demonstrated a simple new method to synthesize 1D nanostructures of TiO_2 via the reaction between the vapor of $TiCl_4$ and the reactive template Na@AAO. By controlling the reaction and annealing temperatures, the structure and the morphology can be adjusted. In theory, replacing O_2 in the oxidation step by other reactive gases could be applied to prepare 1D structures of other Ti containing materials. Investigation is in progress.

Acknowledgement

References

[1] U. Bach, D. Lupo, P. Comte, J.E. Moser, F. Weisörtel, J. Salbeck, H. Spreitzer, M. Grätzel, Nature 395 (1998) 583.
[2] Z.-R. Tian, W. Tong, J.-Y. Wang, N.-G. Duan, V.V. Krishnan, S.L. Suib, Science 276 (1997) 926.
[3] Y. Zhu, J. Shi, Z. Zhang, C. Zhang, X. Zhang, Anal. Chem. 74 (2002) 120.
[4] R.A. Caruso, J.H. Schattka, A. Greiner, Adv. Mater. 13 (2001) 1577.
[5] S. Kobayashi, K. Hanabusa, N. Hamasaki, M. Kimura, H. Shirai, Chem. Mater. 12 (2000) 1523.
[6] P.D. Cozzoli, A. Kornowski, H. Weller, J. Am. Chem. Soc. 125 (2003) 14539.
[7] S. Yoo, S.A. Akbar, K.H. Sandhage, Adv. Mater. 16 (2004) 260.
[8] D. Li, Y. Xia, Nano Lett. 3 (2003) 555.
[9] T. Kasuga, M. Hiramatsu, A. Hoson, T. Sekino, K. Niihara, Adv. Mater. 11 (1999) 1307.
[10] Z.R. Tian, J.A. Voigt, J. Liu, B. Mckenzie, H. Xu, J. Am. Chem. Soc. 125 (2003) 12384.
[11] H.G. Yang, H.C. Zeng, J. Phys. Chem. B 108 (2004) 819.
[12] B.B. Lakshmi, P.K. Dorhout, C.R. Martin, Chem. Mater. 9 (1997) 857.
[13] B.B. Lakshmi, C.J. Patrissi, C.R. Martin, Chem. Mater. 9 (1997) 2544.
[14] Y. Lei, L.D. Zhang, G.W. Meng, G.H. Li, X.Y. Zhang, C.H. Liang, W. Chen, S.X. Wang, Appl. Phys. Lett. 78 (2001) 1125.
[15] M. Zhang, Y. Bando, K. Wada, J. Mater. Sci. Lett. 20 (2001) 167.
[16] S.J. Limmer, S. Seraji, Y. Wu, T.P. Chou, C. Nguyen, G. Cao, Adv. Funct. Mater. 12 (2002) 59.
[17] T. Peng, A. Hasegawa, J. Qiu, K. Hirao, Chem. Mater. 15 (2003) 2011.
[18] X.Y. Zhang, L.D. Zhang, W. Chen, G.W. Meng, M.J. Zheng, L.X. Zhao, Chem. Mater. 13 (2001) 2511.
[19] P. Hoyer, Langmuir 12 (1996) 1411.
[20] S.M. Liu, L.M. Gan, L.H. Liu, W.D. Zhang, H.C. Zeng, Chem. Mater. 14 (2002) 1391.
[21] I.-S. Park, S.-R. Jang, J.S. Hong, R. Vittal, K.-J. Kim, Chem. Mater. 15 (2003) 4633.
[22] A.-P. Li, F. Müller, A. Birner, K. Nielsch, U. Gösele, Adv. Mater. 11 (1999) 483.
[23] A.P. Li, F. Müller, A. Birner, K. Nielsch, U. Gösele, J. Appl. Phys. 84 (1998) 6023.
[24] L.-S. Wang, C.-Y. Lee, H.-T. Chiu, Chem. Commun. (2003) 1964.
[25] S.P.S. Porto, P.A. Fleury, T.C. Damen, Phys. Rev. 154 (1967) 522.
[26] R.J. Betsch, H.L. Park, W.B. White, Mater. Res. Bull. 26 (1991) 613.
[27] H.Y. Zhu, Y. Lan, X.P. Gao, S.P. Ringer, Z.F. Zheng, D.Y. Song, J.C. Zhao, J. Am. Chem. Soc. 127 (2005) 6730.
[28] Reaction-Web, Facility for the Analysis of Chemical Thermodynamics, CRCT, École Polytechnique de Montréal, Montréal. http://www.crct.polymtl.ca/fact/.